Journal of Inflammation Research

Dovepress
Taylor & Francis Group

Open Access Full Text Article

ORIGINAL RESEARCH

Integrated Metabolomics and Transcriptomics Analyses Reveal Metabolic Changes in Primary Angiitis of the Central Nervous System

Ping Lu[1], Lingyun Cui[1], Lulin Zhang[1], Huabing Wang[1], Linlin Yin[1,2], Decai Tian[1,2,*], Xinghu Zhang[1,*]

[1]Center for Neurology, Beijing Tiantan Hospital, Capital Medical University, Beijing, 100070, People's Republic of China; [2]China National Clinical Research Center for Neurological Diseases, Beijing, 100070, People's Republic of China

*These authors contributed equally to this work

Correspondence: Xinghu Zhang, Decai Tian; Center for Neurology, Beijing Tiantan Hospital, Capital Medical University, No. 119, South Fourth Ring Road West, Beijing, 100070, People's Republic of China, Tel +861059976585, Email xhzhtiantan@hotmail.com; decaitian@hotmail.com

Purpose: Metabolic characterization of primary angiitis of the central nervous system (PACNS) is crucial for understanding the disease pathogenesis and progression mechanisms, but it has not been reported in patients. This study aimed to explore changes in the plasma metabolome during the active and remission phases of PACNS and identify potential biomarkers.

Methods: We collected plasma samples from 35 patients with PACNS during the active and remission phases and 22 samples from patients with non-inflammatory disease as controls. Liquid and gas chromatography-mass spectrometry were used to analyze 63 plasma samples from 57 patients metabolically. Meanwhile, we cross-validated the metabolomics results with brain tissue transcriptomic data from comprehensive gene expression databases, enhancing the reliability of our conclusions.

Results: A total of 3,233 metabolites were identified. Enrichment analysis showed significant changes in lactate/amino acid/glycerol–pyruvic–tricarboxylic acid, glycerophospholipid/sphingolipid-membrane metabolism, lysine/tryptophan-essential amino acid metabolism, and uracil metabolism pathways during the active phase of PACNS. These findings were confirmed in both the remission phase of PACNS patients and the transcriptomic samples. Meanwhile, metabolic abnormalities in patients with PACNS were observed with benzoxazole, sesquiterpenoid, and octyl-phenolic products, and enrichment of environmental pollutants and their estrogen-like effects. Twelve metabolites, including D-Ribose, 13s-HPODE, and C16 Sphinganine, showed potential diagnostic and therapeutic evaluation value.

Conclusion: Our study identified potential biomarkers and metabolic characteristics of PACNS using integrated metabolomics and transcriptomics approaches. These findings highlight the importance of understanding PACNS from a metabolic perspective and guide future diagnostic and therapeutic strategies.

Keywords: metabolomics, neuroinflammatory disease, PACNS, transcriptomics, disease biomarkers

Introduction

Primary angiitis of the central nervous system (PACNS) is an idiopathic central vasculitis that mainly affects small to medium-sized vessels of the brain, spinal cord, and meninges.[1–3] The global incidence rate is currently unknown, but the Mayo Clinic estimates an annual incidence rate of approximately 2.4 per million in Caucasian Americans.[4] Despite its clinical rarity, PACNS is characterized by frequent relapses and high disability rates, severely affecting the quality of life of patients and increasing the socioeconomic burden.

Recently, substantial progress has been made in exploring the mechanisms underlying PACNS development using transcriptomics and proteomics. The heterogeneity of PACNS has been identified in different pathological subtypes, and the critical role of complement activation in its pathogenesis has been highlighted.[5,6] Autoimmunity is considered the core mechanism driving PACNS, but the generation of immune responses and their role in causing neurological damage remains

Received: 26 October 2024
Accepted: 18 February 2025
Published: 25 February 2025

Graphical Abstract

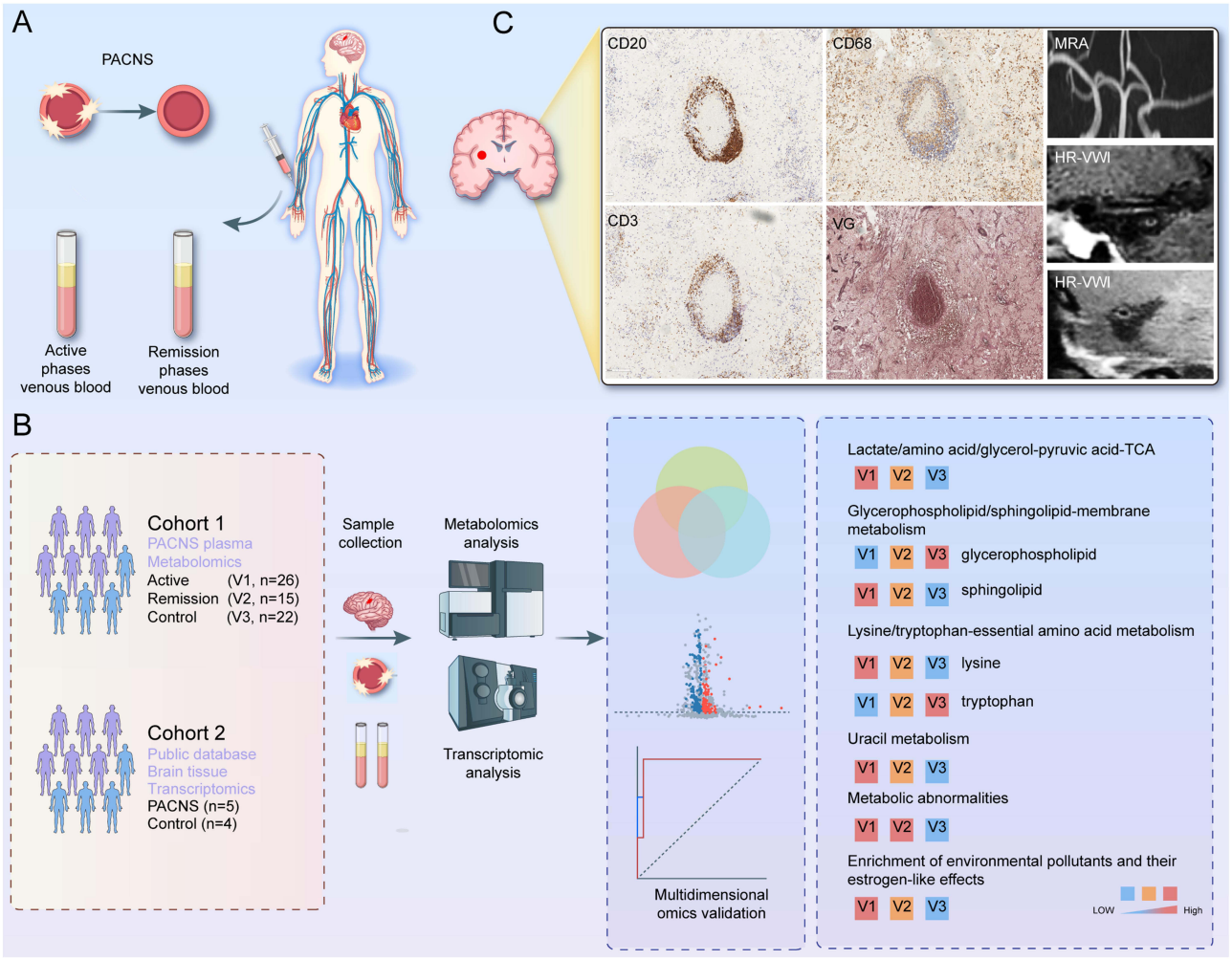

unclear. In addition, the nonspecific clinical manifestations and neuroimaging make the diagnosis of PACNS challenging.[7] Although brain tissue biopsy is the gold standard for diagnosing PACNS, the mild neurological symptoms in the early stages of the disease and symptom relief after initial treatment led to low patient acceptance of the procedure. Additionally, pathologic biopsies can show false negatives.[7,8]

Therefore, to better understand the pathogenesis of PACNS, and improve diagnostic accuracy, it has become urgent to improve existing methods or incorporate new approaches. Blood, as a routine biological diagnostic specimen, is easily accessible through puncture sampling. Metabolites are intermediate or final products produced by organisms during metabolic processes, and they participate in various physiological and biochemical processes.[9] Patients with PACNS exhibit characteristic metabolic changes in their blood that could be used for disease metabolic characterization, enabling earlier diagnosis than that using brain tissue biopsy, thereby avoiding invasive procedures. Regrettably, no studies have been reported on the metabolic characteristics of patients with PACNS. Relevant metabolic research has mainly focused on systemic vasculitis and remains in its early stages.[10–12]

Therefore, in this study, we conducted a comprehensive metabolomic analysis using liquid chromatography-mass spectrometry (LC-MS) and gas chromatography-mass spectrometry (GC-MS) to explore the unique metabolic changes during the active and remission phases of PACNS and identify potential diagnostic biomarkers. Additionally, considering

that changes in the expression of upstream genes may lead to alterations at the metabolic level, we cross-validated the metabolic results with transcriptomic data from public databases to enhance the reliability of our conclusions.

Materials and Methods

Study Patients

This study included two different dimensional cohorts: plasma (Cohort 1) and brain tissue (Cohort 2) of patients with PACNS or non-inflammatory disease (control). In Cohort 1, we collected plasma samples at two-time points from 23 patients with PACNS confirmed by pathological biopsy and 12 patients with PACNS confirmed using angiography. The time points were before treatment initiation (active phase, V1) and during stable treatment (remission phase, V2). However, because of the rarity of PACNS, delayed diagnosis, and high recurrence rate, matching plasma samples from V1 and V2 time points was challenging. We evaluated 41 plasma samples from 35 patients with PACNS, consisting of 26 and 15 from V1 and V2, respectively. Among the 35 patients with PACNS, 10 had matched samples from the V1 and V2 stages. Additionally, we collected 22 plasma samples as controls (V3). In Cohort 2, we utilized transcriptomic information of brain tissues from five patients with PACNS and four control patients from the publicly available Gene Expression Omnibus database (GSE213907) (Graphical Abstract A-B).[6] Details of the demographics of the patients with PACNS (V1 and V2) and controls (V3) are provided in Supplementary Table S1. Clinical characteristics of Cohort 2 have been described in the original literature.

The inclusion criteria for the participants were as follows: all patients with PACNS in Cohort 1 were over 18 years old and met the diagnostic criteria proposed by Calabrese and Mallek in 1988 and Hellmann in 2009.[1,13] Patients had plasma specimens from stage V1 or V2 and were excluded if the specimen was missing. Additionally, all patients underwent comprehensive examinations, including serologic panels for autoantibodies and MRI, to rule out infection, tumors, systemic vasculitis, and other diseases involving the central nervous system during hospitalization. Biopsy specimens needed to present with transmural cell infiltration (Graphical Abstract C). "Untreated" participants were defined as those who received no steroids or immunosuppressive therapy at V1. "Stable period" was defined as no recurrence or worsening of neurological symptoms within 6 months before or after V2 and no evidence of new lesions on neuroimaging. Patients with non-inflammatory diseases in Cohort 1 were mainly patients with angiographically confirmed venous sinus stenosis and healthy individuals.

Sample Collection and Preparation

Blood was collected from patients in the early morning after admission, typically in a fasting state. Plasma samples were immediately centrifuged (1200 ×*g*, 4°C, 10 min) within 30 min of collection to avoid hemolysis, and only non-hemolyzed samples were subsequently analyzed. Samples were then stored at −80°C and thawed on ice on the day of analysis. Detailed information on sample preparation for dual-platform metabolomics is provided in Supplementary Data S1.1, while information on major reagents and instruments is listed in Supplementary Data S1.2 and S1.3.

Data Collection and Metabolite Identification

Experiments were conducted using Waters ACQUITY ultra-high-performance LC (UPLC) I-Class plus/Thermo quadrupole-electrostatic (QE) UPLC–tandem mass spectrometry (MS/MS) and Agilent 7890B-5977A GC–MS systems. Full-spectrum metabolomics with MS-DIAL qualitative software was used for qualitative and relative quantitative analysis of raw data, followed by standardized preprocessing. Compound identification was based on multiple dimensions including retention time, exact mass, MS/MS fragmentation, and isotope distribution using databases such as The Human Metabolome Database (HMDB), Lipidmaps (v2.3), METLIN database, and LuMet-Animal3.0 local database. Detailed information on data collection and metabolite identification is provided in Supplementary Data S1.4.

Data Quality Control and Differential Metabolite Identification

The protocol used for processing metabolomics data is described in Supplementary Data S1.5. The Variable Important in Projection (VIP) was used to assess the impact strength and interpretability of metabolite expression patterns on sample

classification. Unsupervised principal component analysis (PCA), partial least squares discriminant analysis (PLS-DA), volcano plots, and heat maps were employed for qualitative and quantitative data analysis and visualization to understand inter-group metabolic differences and identify differentially expressed metabolites. The selection criteria were P-value < 0.05 and VIP > 1.

Data Quality Control and Differential Gene Identification

The gene count data for each sample in the transcriptome were normalized using DESeq2 software (Base Mean values were used to estimate gene expression). Differential expression was assessed using the negative binomial distribution test, with a significance threshold of P-value < 0.05 and | log2(fold change (FC)) | ≥ 1.

Statistical Analysis

Continuous variables are expressed as mean ± standard deviation or median (range), while categorical variables are shown as frequency and percentage. To compare continuous variables between groups, either analysis of variance or the Wilcoxon rank-sum test was applied, and the Pearson chi-square test was used for categorical variables. The Kyoto Encyclopedia of Genes and Genomes (KEGG) database was used to annotate differential metabolites and identify relevant metabolic pathways. Using the R package Mfuzz, fuzzy clustering analysis was performed. Subject operating characteristic curves (ROC) were used to assess the diagnostic value of metabolites for PACNS. Graphs were generated using GraphPad Prism software 8(GraphPad Software, San Diego, CA, USA).

Results

Inter-Group Metabolomics Product Identification and Quality Assessment

Internal standards and quality control samples were used to ensure that the metabolic profiling results were stable and reliable. In total, 3233 metabolites were detected, and representative LC-MS and GC–MS chromatograms are provided in Supplementary Figure S1. We identified distinct plasma metabolic profiles among patients in the V1 and V2 phases of PACNS and those in the V3. Compared to V3 patients, V1 patients showed significant differences in 231 metabolites (106 upregulated and 125 downregulated). Upon reaching the V2 phase, 178 metabolites showed changes compared to levels in the V1 phase, with 72 upregulated and 106 downregulated. Additionally, compared to V3, in the V2 phase, 207 metabolites showed changes, consisting of 99 upregulated and 108 downregulated metabolites (Figure 1A). Venn diagram analysis revealed that 112 (V1 vs V3 and V2 vs V1) and 110 (V1 vs V3 and V2 vs V3) metabolites were shared between the groups, respectively (Figure 1B).

PLS-DA demonstrated significant discrimination among the three groups with good quality parameters and predictive ability (Figure 1C). This observation highlighted that the metabolic changes were more pronounced among the V1 vs V3 and V2 vs V3 groups than they were between V1 and V2. Orthogonal PLS-DA and unsupervised PCA results are provided in Supplementary Figures S2 and S3. To validate the effectiveness of the model, permutation testing of supervised methods was conducted using n = 200 permutations (Supplementary Figure S4).

KEGG Enrichment of Differentially Expressed Metabolites

Compared to those in V3, the top 10 upregulated KEGG metabolic pathways with the smallest P-value in V1 were primarily enriched in energy (including citrate cycle, glyoxylate, and dicarboxylate) metabolism. In addition, amino acid (including pyruvate, arginine biosynthesis, glutamate, butanoate, D-amino acids, lysine degradation, and isoleucine) and glycerophospholipid metabolism pathways were also primarily enriched. Downregulated metabolites were mainly enriched in linoleic acid, glycerophospholipids, tryptophan, galactose, and glycosylphosphatidylinositol (GPI)-anchor biosynthesis pathways.

Analysis of metabolites in V2 revealed that the metabolic pathways of the citrate cycle, butanoate, D-amino acids, lysine degradation, isoleucine, and glycerophospholipid, which were upregulated in V1, were downregulated in V2. In contrast, arginine and glutamate metabolism pathways were more significantly upregulated in V2 than they were in V1. Furthermore, pathways associated with downregulated linoleic acid, glycerophospholipids, and GPI-anchor biosynthesis in V1 were significantly upregulated in V2 (Figure 2A–D).

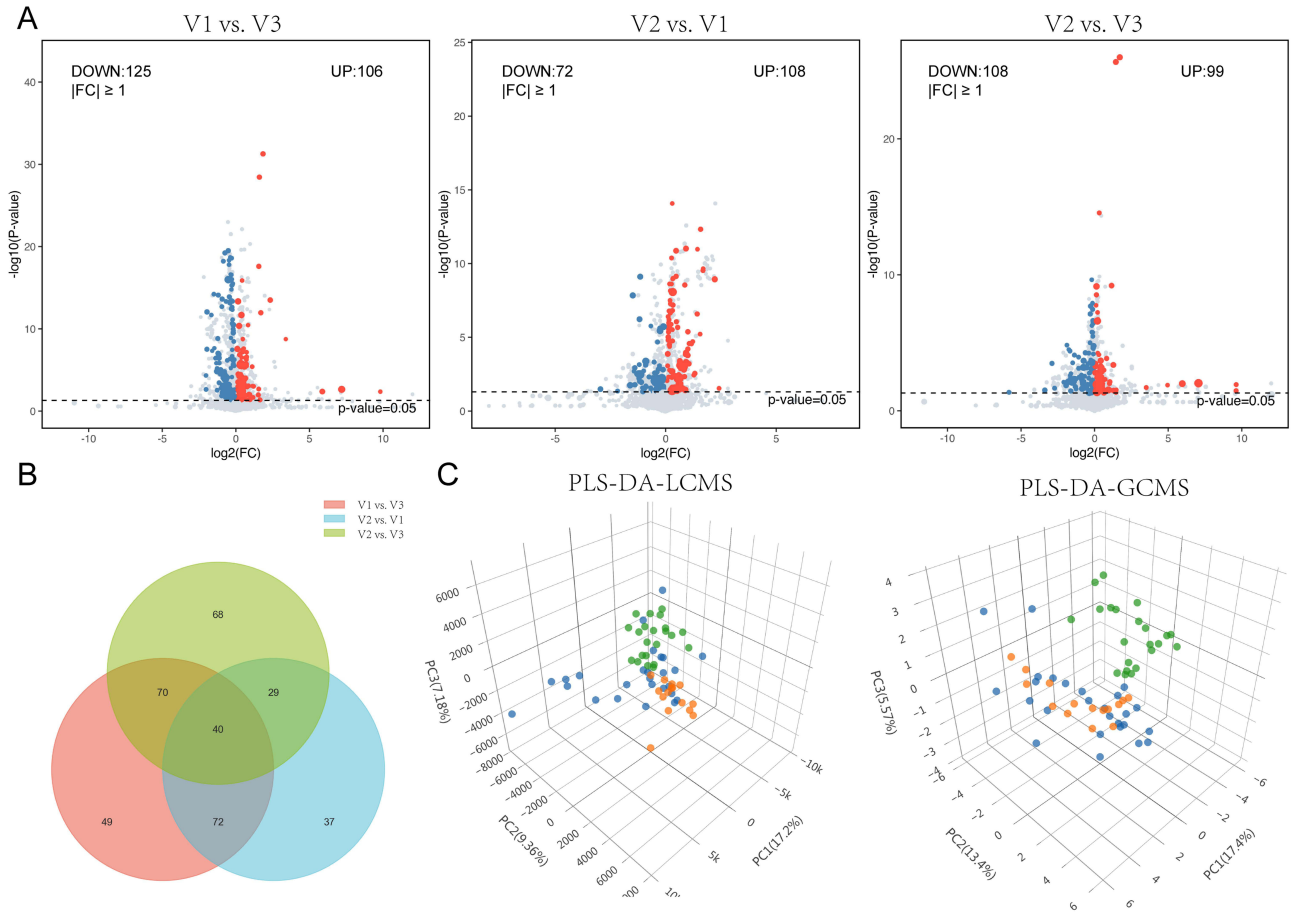

Figure 1 Inter-group metabolomics product identification and quality assessment. (**A**) Heatmap illustrating inter-group differences in metabolites; p-values were calculated using *t*-test or Wilcoxon test with selection criteria of P < 0.05 and VIP > 1. Red and blue dots represent upregulated and downregulated metabolites, respectively. (**B**) Venn diagram depicting inter-group differential metabolites. (**C**) Partial least squares discriminant analysis (PLS-DA) results of inter-group LC–MS and GC–MS data; blue, Orange, and green dots correspond to V1, V2, and V3 groups, respectively.

Product Identification and KEGG Enrichment of Differentially Expressed Genes

In Cohort 2, we evaluated brain tissue transcriptomic information from five patients with PACNS and four control patients, and 844 differentially expressed genes were detected, with 741 upregulated and 103 and downregulated genes. To further explore the relationship between genes and metabolism, we compared these differentially expressed genes with the genes in the top 10 KEGG metabolic pathways mentioned above, identifying potential regulatory genes. Ultimately, our analysis revealed 15 differentially expressed genes enriched in the KEGG metabolic pathways mentioned above; these genes were lactate dehydrogenase D (LDHD), phosphoenolpyruvate carboxykinase 1 (PCK1), alanine–glyoxylate aminotransferase (AGXT), alcohol dehydrogenase 6 (class V) (ADH6), ADH4, phospholipase A2 group IIA (PLA2G2A), PLA2G4E, carboxyl ester lipase (CEL), monoacylglycerol O-acyltransferase 3 (MOGAT3), delta 4-desaturase, sphingolipid 2 (DEGS2), indoleamine 2,3-dioxygenase 1 (IDO1), aldehyde dehydrogenase 8 family member A1 (ALDH8A1), tryptophan hydroxylase 1 (TPH1), dopa decarboxylase (DDC), and estrogen receptor beta (ESR2) (Figure 2E and F).

Integration of Differentially Expressed Metabolites and Genes Reveals Unique Metabolic Processes During the Active Phase in Patients with PACNS

Lactate/Amino Acid/Glycerol–Pyruvate–Tricarboxylic Acid (TCA) Pathway

As shown in Figure 3A–D, compared to V3 patients, V1 patients exhibited significant increases in pyruvate, fumarate, and malate levels, whereas citrate levels decreased markedly, indicating enhanced TCA pathway activity. The TCA cycle serves as a key node linking lactate, amino acid, and glycerophosphate metabolism. Integrated transcriptomic analysis

https://doi.org/10.2147/JIR.S503058

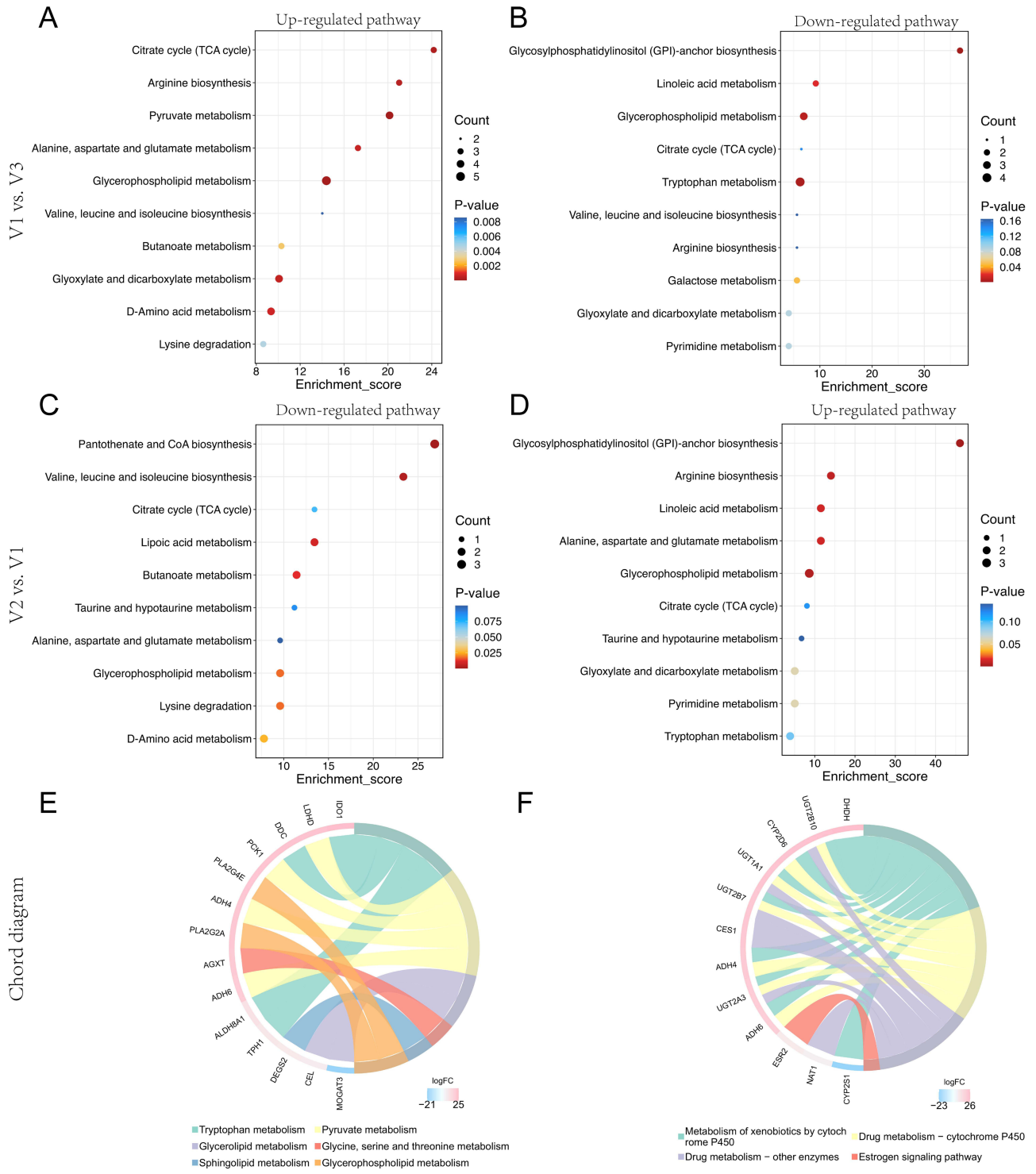

Figure 2 KEGG enrichment of differentially expressed metabolites and genes. (**A** and **B**) Bubble plot. Top 10 upregulated and downregulated KEGG metabolic pathways between V1 vs V3. (**C** and **D**) Bubble plot. Top 10 upregulated and downregulated KEGG metabolic pathways between V2 vs V1. The larger the bubble, the more differential metabolites are included in the pathway. The enrichment p-value changes with the bubble color from blue to red; (**E** and **F**) The differential genes obtained from Cohort 2 were compared with the genes in the top 10 KEGG metabolic pathways mentioned above, identifying potential regulatory genes. The KEGG chord diagram illustrates the enriched pathways of these genes.

revealed increased mRNA expression of LDHD, PCK1, AGXT, ADH6, and ADH4, which are related to pyruvate metabolism. This finding suggests that pyruvate originating from lactate, amino acid, and glycerol metabolism may act as a critical regulatory factor that enhances the TCA cycle pathway in patients with PACNS. LDHD catalyzed the

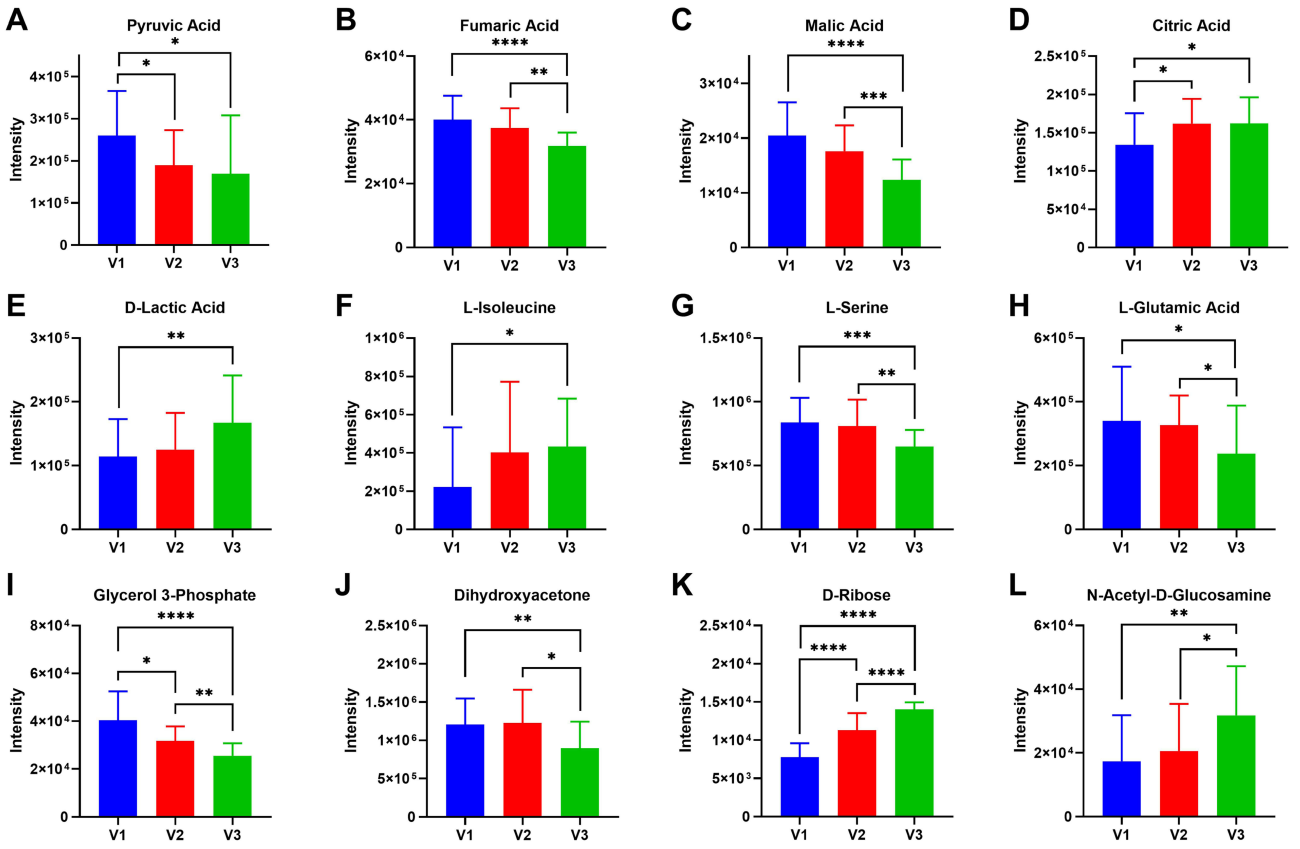

Figure 3 The specific biological processes of PACNS. (**A**–**L**) Changes in metabolites of lactate/amino acid/ glycerol - pyruvate -TCA pathway among V1, V2, and V3 groups. Non-paired *t*-test or Wilcoxon test calculation, with significance indicated as follows: *P < 0.05, **P < 0.01, ***P < 0.001, ****P < 0.0001.

bidirectional conversion of pyruvate and D-lactate (forward in glycolysis and backward in gluconeogenesis), as shown in Figure 3E, with significantly lower D-lactate levels in V1 than in V3 group. This was indicative of inhibited glycolysis, corroborated by the regulation of PCK1 as a rate-limiting enzyme in gluconeogenesis.

Amino acids can undergo gluconeogenic transformation to pyruvate, contributing to the TCA cycle. Integrated transcriptomic analysis revealed that increased AGXT mRNA expression facilitated the transamination between L-serine and pyruvate, thereby contributing to gluconeogenesis in L-serine metabolism. As depicted in Figure 3F–H, compared to V3 patients, V1 patients showed decreased levels of the essential amino acid isoleucine and increased non-essential amino acids L-serine and L-glutamine, indicating an enhancement of amino acid gluconeogenesis pathways. Glycerophosphate and dihydroxyacetone phosphate can undergo enzymatic interconversion, serving as chemical intermediates in glycolytic and/or gluconeogenic pathways. As shown in Figure 3I and J, compared to V3 patients, V1 patients exhibited significant increases in glycerol 3-phosphate and dihydroxyacetone phosphate levels. Additionally, the levels of D-ribose and N-acetyl-D-glucosamine as energy-regulatory substances were significantly increased in V1 patients (Figure 3K and L).

Glycerophospholipid/Sphingolipid–Membrane Metabolism Pathway

In patients with PACNS, increased mRNA levels of PLA2G2A, PLA2G4E, CEL, MOGAT3, and DEGS2 primarily regulate phospholipid metabolism in biological membranes, catalyzing the release of free fatty acids (such as the essential fatty acid linoleic acid) and lysophospholipid. Compared to V3 patients, V1 patients showed significant alterations in various glycerophospholipids (mainly phosphatidylethanolamines and phosphatidylcholines), with notable increases in lysophospholipid levels (Figure 4A–D). Additionally, compared to V3 patients, V1 patients exhibited significantly elevated levels of sphingosine-1-phosphate (S1P) and significant decreases in its metabolites such as O-phosphoethanolamine and the linoleic acid metabolite 13-HPODE (Figure 4E–G). The changes observed in these metabolites may reflect the dynamic disruption and repair of biological membranes in patients with PACNS.

https://doi.org/10.2147/JIR.S503058

Lysine/Tryptophan-Essential Amino Acid Metabolic Pathway

We observed significant and opposite changes in levels of various intermediate metabolites that are involved in lysine and tryptophan metabolism. As shown in Figure 4H–J, compared to in V3 patients, the levels of intermediate metabolites of lysine (cadaverine, pipecolic acid, and aminoadipic acid) significantly increased in V1 patients. Of these, cadaverine and pipecolic acid mainly originate from the bacterial enzymatic metabolism of lysine in the gut, whereas aminocaproic acid inhibits tryptophan metabolite production.[14] Correspondingly, compared to V3 patients, the levels of tryptophan metabolites serotonin, melatonin, and skatole were reduced in V1 patients (Figure 4K–M). Meanwhile, transcriptomic analysis revealed a significant increase in the mRNA levels associated with serotonin and melatonin synthesis (TPH1 and DDC) and metabolism (IDO1) (Figure 2E).

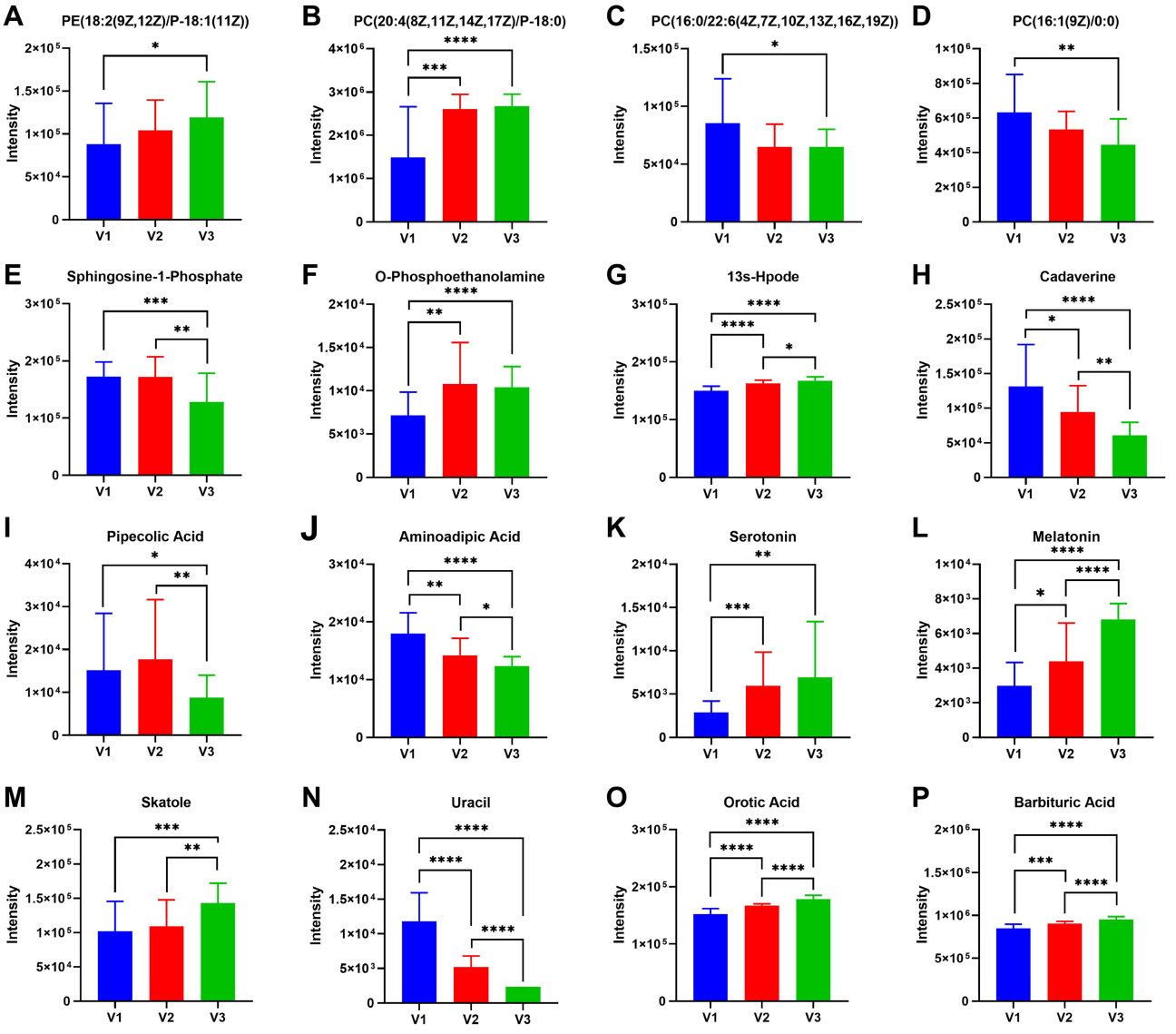

Figure 4 The specific biological processes of PACNS. (**A**–**G**) Changes in metabolites of glycerophospholipid/sphingolipid-biofilm metabolic pathway among V1, V2, and V3 groups of patients with PACNS; (**H**–**M**) Changes in metabolites of lysine/tryptophan-essential amino acid metabolic pathway among the three groups; (**N**–**P**) Changes in metabolites of uracil metabolism pathway among the three groups. Non-paired *t*-test or Wilcoxon test calculation, with significance indicated as follows: *P < 0.05, **P < 0.01, ***P < 0.001, ****P < 0.0001.

https://doi.org/10.2147/JIR.S503058

Uracil Metabolism Pathway

We found that the uracil synthesis pathway was enhanced in patients with PACNS (Figure 4N–P). Compared to those in V3 patients, uracil levels were significantly elevated in V1 patients, whereas levels of the synthesized substances, orotate and barbituric acid, were significantly reduced.

Biological Markers for the PACNS Acute and Remission Phases

To better differentiate patients with PACNS from those with non-inflammatory diseases, and considering the changes in metabolites during the acute and remission phases, we cross-compared V1 vs V3, V2 vs V1, and V2 vs V3. This process identified 222 differential metabolites, including 40 that were common across different groups, indicating that 182 significantly different metabolites overlapped. We used fuzzy clustering analysis to categorize these 182 metabolites into six clusters, illustrating their differential change trends (Figure 5A). Subsequently, we analyzed metabolites with inter-group ROC curve area ≥ 0.95.

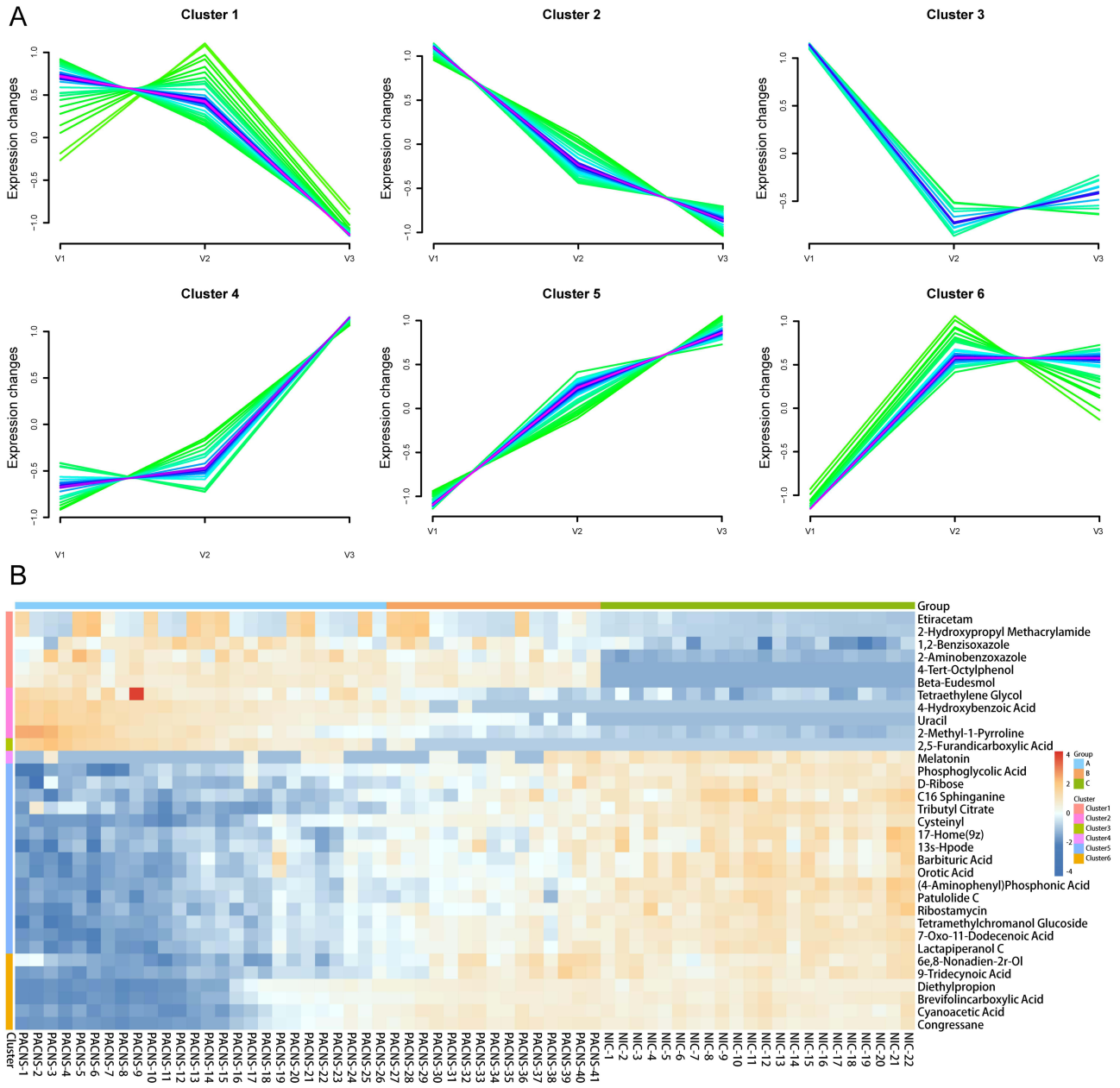

Figure 5 Different expression patterns of metabolites in plasma during different stages of PACNS. (**A**) Fuzzy clustering analysis of 182 metabolites, illustrating their differential change trends. (**B**) Heatmap analysis showing the 33 metabolites involved in KEGG enrichment.

https://doi.org/10.2147/JIR.S503058

In the V1 vs V3 group, 58 metabolites met this criterion, including D-ribose, 13s-HPODE, melatonin, uracil, orotic acid, and barbituric acid, which was evaluated in the KEGG enrichment analysis. Moreover, 20 and 13 metabolites met the criterion in the V2 vs V1 and V2 vs V3 group comparisons, respectively, with 27 metabolites in common with the 58 metabolites in the V1 vs V3 group. Ultimately, we analyzed 33 metabolites, which included the six metabolites that were identified in the KEGG enrichment analysis and the 27 metabolites that were shared among different groups (Figure 5B).

Abnormal Metabolism of Benzoxazole, Sesquiterpenes, and Octyl-Phenolic Products

Six metabolites showing significantly higher abundances in both V1 and V2 than they did in V3 could be grouped into Cluster 1. Furthermore, no significant difference was observed in abundance between V1 and V2. Among the metabolites, changes in etiracetam and 2-hydroxypropyl methacrylamide, metabolites of the anti-epileptic drug levetiracetam and its nano-encapsulated particles, were highly correlated, which further validates the reliability of results obtained from our metabolomics analysis. Additionally, two benzisoxazole metabolites, 1.2-benzisoxazole and 2-aminobenzoxazole, and exogenous beta-eudesmol and 4-tert-octylphenol, showed abnormalities in patients with PACNS. As shown in Figure 2F, the transcriptional activity of the hepatic enzyme system is enhanced in patients with PACNS, with UGT2B7 playing a crucial role in detoxifying 4-tert-octylphenol.[15]

Enrichment and Estrogen-Like Effects of Environmental Pollutants

Five metabolites showing the highest abundance in V1 could be classified into Clusters 2 and 3, and their abundance gradually decreased in V2 and V3. Furthermore, Cluster 2 primarily consisted of environmental pollutants, including tetraethylene glycol, 4-hydroxybenzoic acid, 2-methyl-1-pyrroline, and 2.5-furan dicarboxylic acid. Among them, 4-hydroxybenzoic acid exhibits estrogenic effects in vivo.[16] In addition, we discovered that in Cluster 1, the estrogen-like chemical 4-tert-octylphenol, widely used as a plasticizer and surfactant, showed significantly elevated levels in patients with PACNS.[17] The transcriptomic data revealed a significant upregulation of estrogen receptors (ESR2) in patients with PACNS (Figure 2F).

Downregulation of Multiple Metabolites

We identified 21 metabolites, which were grouped into Clusters 3–6 and showed significantly decreased abundance in V1 and gradually increasing abundance in V2 and V3. This included the five KEGG-enriched metabolites: D-ribose, 13s-HPODE, melatonin, orotic acid, and barbituric acid. Among the additional 16 metabolites, we observed decreased levels of fatty acids (such as 9-tridecynoic acid, 7-oxo-11-dodecenoic acid, and 17-home[9z]) and sphinganines (such as C16 sphinganine), which are related to energy metabolism and biomembrane components.

Combined KEGG Enrichment Analysis Identified Potential Markers for PACNS

Based on the six metabolic pathways previously identified, we selected 12 known metabolites from 33 metabolites as potential biomarkers for PACNS. The area under the ROC curve for these metabolites was all >0.95, with $P < 0.05$, balancing both diagnostic accuracy and therapeutic effectiveness. These selected markers included 2-aminobenzoxazole, 1.2-benzisoxazole, beta-eudesmol, and 4-tert-octylphenol as abnormal metabolites; D-ribose from the lactate/amino acid/glycerol–pyruvic acid–TCA pathway; 13s-HPODE and C16 sphinganine from the glycerophospholipid and sphingolipid-biomembrane pathways; melatonin from the lysine and tryptophan-essential amino acid pathways; uracil, orotic acid, and barbituric acid from the pyrimidine metabolism pathway; and 4-hydroxybenzoic acid from the estrogen pathway (Figure 6A–L).

Discussion

This study, to the best of our knowledge, provides a novel comprehensive metabolic characterization of patients with PACNS, which is crucial for understanding the onset and progression of the disease. Our findings indicate significant alterations in lactate/amino acid/glycerol–pyruvic–TCA cycle, glycerophospholipid/sphingolipid-membrane metabolism, arginine/tryptophan-essential amino acid metabolism, and uracil metabolism pathways during the active phases in these patients. Additionally, we observed metabolic abnormalities of benzoxazoles, sesquiterpenes, and octyl-phenolic and enrichment of environmental pollutants and their estrogenic effects in patients with PACNS. Twelve potential biological

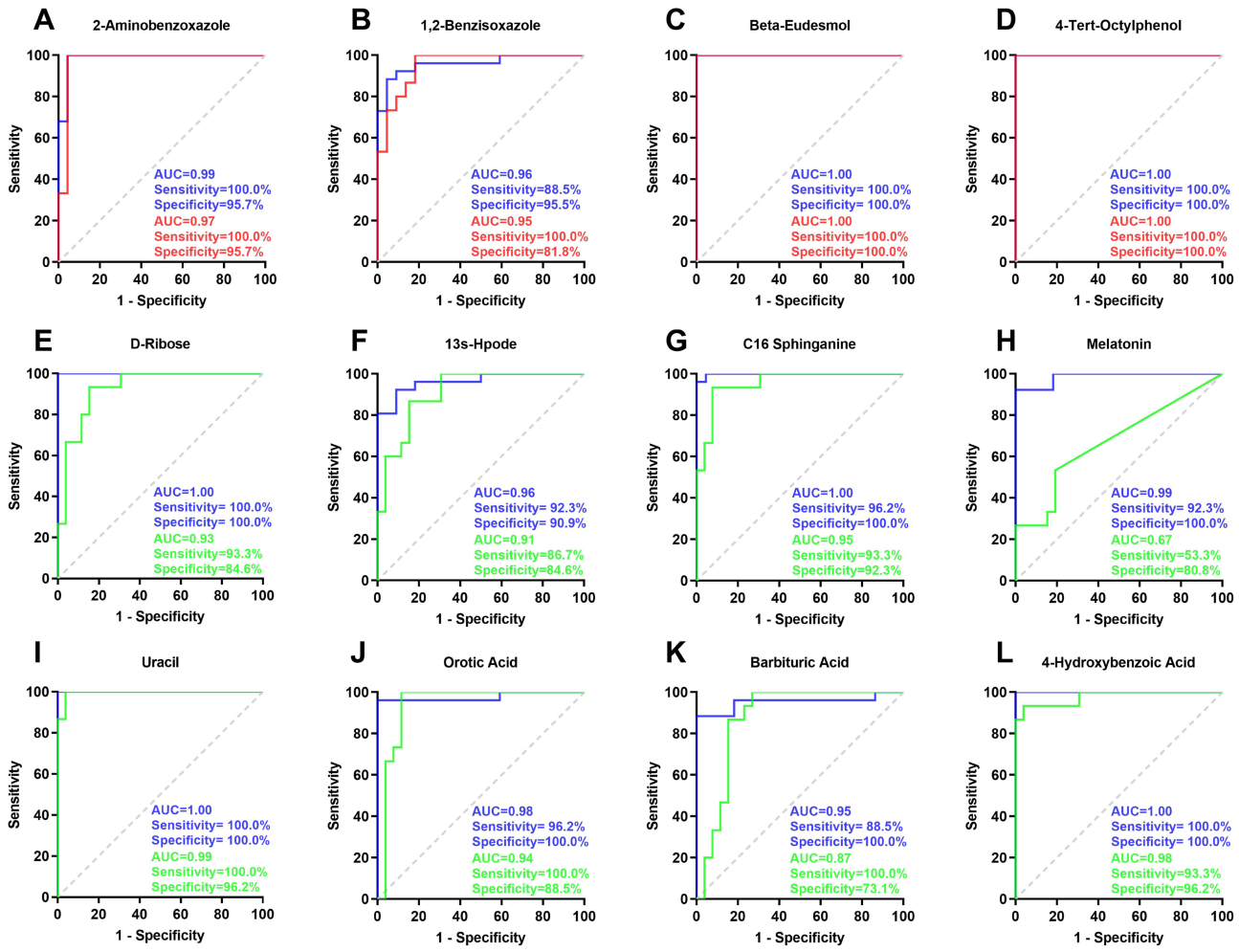

Figure 6 Diagnostic and therapeutic assessment value of 12 plasma metabolites analyzed by area under the ROC curve (**A–L**). Blue, red, and green colours represent V1 vs V3, V2 vs V3, and V1 vs V2, respectively.

markers with diagnostic and therapeutic evaluation value were identified, covering the identified altered metabolic pathways.

In patients with PACNS, inflammatory cell infiltration into small vessel walls disrupts the normal blood–brain barrier structure, increasing permeability and providing critical conditions for the exchange of metabolic products between inflammatory tissue and the local blood environment.[18] Enhanced pathways, including the TCA cycle, amino acids, phospholipids, and uracil metabolism, may reflect increased energy and metabolic demands during the active phases of PACNS. Stroke-like ischemic manifestations and lymphocyte proliferation may contribute to the increased demand for energy and metabolic activities during the active disease phase to maintain inflammatory responses and tissue repair.[19,20] As the disease enters a stable phase, inflammation subsides and tissue repair diminishes, leading to overall restoration of the identified altered metabolic pathways to a non-inflammatory disease state.

Enhancement of the TCA cycle metabolic pathway also occurs in other diseases. Patients with anti-neutrophil cytoplasmic antibody-associated vasculitis, acute ischemic stroke, and glioma primarily rely on glycolysis.[19,21] However, in our study, we found that patients with PACNS mainly depend on gluconeogenesis as their primary energy supply pathway, which is possibly related to lesion location and the subacute course. The brain has the highest energy demand of all organs, and neurons preferentially derive energy from glucose; however, the brain tissue lacks glycogen stores. Under prolonged chronic inflammatory stimulation, PACNS forms a predominantly gluconeogenic energy supply system.

https://doi.org/10.2147/JIR.S503058

Amino acids involved in various gluconeogenic pathways also play important roles in protein synthesis and immune regulation. For example, isoleucine is an essential amino acid that may attenuate inflammatory mediator release and regulate oxidative stress, thereby alleviating inflammatory responses.[22] Our study shows a significant decrease in isoleucine levels in patients with PACNS, possibly attributed to inadequate exogenous supplementation and increased endogenous consumption. Furthermore, D-ribose and N-acetyl-D-glucosamine, two energy regulators, play important roles in maintaining cellular energy levels and regulating cellular responses to hormones such as insulin.[23,24]

Phospholipids, which are major components of the cell membrane, are divided into glycerophospholipids and sphingolipids and play unique and complex roles in inflammatory signaling. Attacks by free radical-mediated glycerophospholipid produce platelet-activating factor-like lipids, exerting acute inflammatory and delayed immune-suppressive effects.[25] Sphingosine-1-phosphate, a bioactive metabolite of sphingolipids, plays a crucial role in regulating the movement of lymphocytes from the thymus or secondary lymphoid organs into circulation.[26,27] Moreover, low levels of sphingosine-1-phosphate in blood promote endothelial inflammation, damage the endothelial barrier, and affect vascular genesis.[28] In our study, patients with PACNS showed decreased glycerophospholipids and increased sphingosine-1-phosphate levels, which may play a critical role in blood–brain barrier repair, inflammation suppression, and vascular genesis.

Previous studies have shown that a decrease in tryptophan levels may lead to the progression of Kawasaki disease symptoms, and supplementation with tryptophan has been demonstrated to be beneficial.[11,29] Additionally, tryptophan is a precursor of serotonin and melatonin and plays a role in regulating the release of inflammatory mediators. At the same time, IDO1 is involved in the aforementioned synthesis pathways and is considered a target gene for regulating excessive immune responses in human autoimmune diseases.[30] Similarly, our study revealed elevated IDO1 mRNA levels and a deficiency in tryptophan and its metabolites in patients with PACNS; however, its therapeutic efficacy under these conditions needs further validation. Conversely, another essential amino acid, lysine, and its metabolites showed significantly increased levels in patients with PACNS, including cadaverine, which is harmful to the human body. Among them, aminoadipic acid has been shown to inhibit the protective tryptophan metabolite, kynurenic acid, in brain tissue slices.[14] This finding may help explain the increased mRNA expression levels of the rate-limiting enzymes IDO1 and ALDH8A1 in the canine uric acid metabolic pathway as observed in the transcriptomics analysis. In contrast, no significant differences were found in canine uric acid levels in the metabolomics analysis.

The serum of patients with active anti-neutrophil cytoplasmic antibody-associated vasculitis and glioma have been shown to present elevated levels of metabolites involved in nucleotide synthesis, similar to our findings.[31,32] We observed an increase in uracil levels in patients with PACNS. However, unlike that in glioma, the intermediate orotic acid in its synthesis pathway showed an opposite trend.[33] Previous studies have shown that excessive orotic acid feeding is associated with tumor formation.[34,35] The decreased orotic acid levels in PACNS may be a potential biomarker that can help in distinguishing it from glioma. Finally, benzoxazole and sesquiterpene compounds may play a role in inhibiting proliferation and immune responses.[36,37] 4-hydroxybenzoic acid and 4-tert-octylphenol may significantly upregulate estrogen receptors through estrogen-like effects.[16,17] These findings reveal that environmental factors may play a role in the pathogenesis of PACNS.[38]

In summary, in this study we used a multidimensional approach combining plasma metabolomics and brain tissue transcriptomics to identify the potential biomarkers and metabolic characteristics of PACNS for the first time, filling a gap in this field. However, the study has some limitations that are worth mentioning. First, although samples were collected for 6 years, the low incidence rate of PACNS resulted in a limited sample size for biomarker screening. Additionally, external validation is lacking for the applicability of the biomarkers for clinical diagnosis. We are currently continuing sample collection and plan to expand the sample size in future studies to further validate our findings.

Conclusion

By integrating metabolomics and transcriptomics data, we successfully identified significant metabolic changes between PACNS patients and non-inflammatory disease controls, pinpointed highly accurate biomarkers, and explored potential disease mechanisms. These findings highlight the importance of understanding PACNS from a metabolic perspective and provide valuable guidance for future diagnostic and therapeutic strategies.

Ethics Approval and Informed Consent

This study was approved by the Research Ethics Committee of Beijing Tiantan Hospital, Capital Medical University (KY2017-002) and is in accordance with the Helsinki Declaration (WMA Helsinki Declaration, 2013) and the General Data Protection Regulation. Prior to inclusion in the study, all participants provided informed consent.

Data Sharing Statement

Data are available upon reasonable request. Data will be available to researchers on request for purposes of reproducing the results or replicating the procedure by directly contacting the corresponding author.

Acknowledgment

We thank our patients for participating in this study and all members of the neuroimmunology team for their support.

Author Contributions

All authors made a significant contribution to the work reported, whether that is in the conception, study design, execution, acquisition of data, analysis and interpretation, or in all these areas; took part in drafting, revising or critically reviewing the article; gave final approval of the version to be published; have agreed on the journal to which the article has been submitted; and agree to be accountable for all aspects of the work.

Funding

This work was supported by National Natural Science Foundation of China (No. 82471373, 82271374), Beijing Natural Science Foundation (7212030, 7212029) and Beijing Natural Science Foundation grant (JQ23027).

Disclosure

The authors declare that they have no competing interests in this work.

References

1. Calabrese LH, Mallek JA. Primary angiitis of the central nervous system. Report of 8 new cases, review of the literature, and proposal for diagnostic criteria. *Medicine*. 1988;67(1):20–39. doi:10.1097/00005792-198801000-00002
2. Salvarani C, Brown RD Jr, Christianson TJH, Huston J 3rd, Giannini C, Hunder GG. Long-term remission, relapses and maintenance therapy in adult primary central nervous system vasculitis: a single-center 35-year experience. *Autoimmunity Rev*. 2020;19(4):102497. doi:10.1016/j.autrev.2020.102497
3. de Boysson H, Boulouis G, Aouba A, et al. Adult primary angiitis of the central nervous system: isolated small-vessel vasculitis represents distinct disease pattern. *Rheumatology*. 2017;56(3):439–444. doi:10.1093/rheumatology/kew434
4. Salvarani C, Brown RD Jr, Christianson T, et al. An update of the Mayo clinic cohort of patients with adult primary central nervous system vasculitis: description of 163 patients. *Medicine*. 2015;94(21):e738. doi:10.1097/MD.0000000000000738
5. Mandel-Brehm C, Retallack H, Knudsen GM, et al. Exploratory proteomic analysis implicates the alternative complement cascade in primary CNS vasculitis. *Neurology*. 2019;93(5):E433–E444. doi:10.1212/WNL.0000000000007850
6. Salvarani C, Paludo J, Hunder GG, et al. Exploring gene expression profiles in primary central nervous system vasculitis. *Ann Neurol*. 2023;93(1):120–130. doi:10.1002/ana.26537
7. Nehme A, Lanthier S, Boulanger M, et al. Diagnosis and management of adult primary angiitis of the central nervous system: an international survey on current practices. *J Neurol*. 2023;270(4):1989–1998. doi:10.1007/s00415-022-11528-7
8. Beuker C, Strunk D, Rawal R, et al. Primary angiitis of the CNS: a systematic review and meta-analysis. *Neurol Neuroimmunol Neuroinflamm*. 2021;8(6). doi:10.1212/NXI.0000000000001093.
9. Chen Y, Lu T, Pettersson-Kymmer U, et al. Genomic atlas of the plasma metabolome prioritizes metabolites implicated in human diseases. *Nat Genet*. 2023;55(1):44–53. doi:10.1038/s41588-022-01270-1
10. Liu S, Xu Q, Wang Y, Lv Y, Liu QQ. Metabolomics combined with clinical analysis explores metabolic changes and potential serum metabolite biomarkers of antineutrophil cytoplasmic antibody-associated vasculitis with renal impairment. *PeerJ*. 2023; 11:e15051.
11. Fan X, Li K, Guo X, et al. Metabolic profiling reveals altered tryptophan metabolism in patients with Kawasaki disease. *Front Mol Biosci*. 2023;10:1180537. doi:10.3389/fmolb.2023.1180537
12. Iliou A, Argyropoulou OD, Palamidas DA, et al. NMR-based metabolomics in giant cell arteritis and polymyalgia rheumatica sequential sera differentiates active and inactive disease. *Rheumatology*. 2023: kead590.
13. Birnbaum J, Hellmann DB. Primary angiitis of the central nervous system. *Arch Neurol*. 2009;66(6):704–709. doi:10.1001/archneurol.2009.76
14. Wu HQ, Ungerstedt U, Schwarcz R. L-alpha-aminoadipic acid as a regulator of kynurenic acid production in the hippocampus: a microdialysis study in freely moving rats. *Eur J Pharmacol*. 1995;281(1):55–61. doi:10.1016/0014-2999(95)00224-9

15. Isobe T, Ohkawara S, Tanaka-Kagawa T, Jinno H, Hanioka N. Hepatic glucuronidation of 4-tert-octylphenol in humans: inter-individual variability and responsible UDP-glucuronosyltransferase isoforms. *Arch Toxicol*. 2017;91(11):3543–3550. doi:10.1007/s00204-017-1982-1
16. Lemini C, Silva G, Timossi C, et al. Estrogenic effects of p-hydroxybenzoic acid in CD1 mice. *Environ Res*. 1997;75(2):130–134. doi:10.1006/enrs.1997.3782
17. Olaniyan LWB, Okoh OO, Mkwetshana NT, Okoh AI. Environmental water pollution, endocrine interference and ecotoxicity of 4-tert-octylphenol: a review. *Rev Environ Con Toxicol*. 2020;248:81–109. doi:10.1007/398_2018_20
18. Coisne C, Engelhardt B. Tight junctions in brain barriers during central nervous system inflammation. *Antioxid Redox Signaling*. 2011;15(5):1285–1303. doi:10.1089/ars.2011.3929
19. Geng J, Zhang Y, Li S, et al. Metabolomic profiling reveals that reprogramming of cerebral glucose metabolism is involved in ischemic preconditioning-induced neuroprotection in a rodent model of ischemic stroke. *J Pro Res*. 2019;18(1):57–68. doi:10.1021/acs.jproteome.8b00339
20. Marchingo JM, Sinclair LV, Howden AJ, Cantrell DA. Quantitative analysis of how Myc controls T cell proteomes and metabolic pathways during T cell activation. *Elife*. 2020;9. doi:10.7554/eLife.53725
21. Jelluma N, Yang X, Stokoe D, Evan GI, Dansen TB, Haas-Kogan DA. Glucose withdrawal induces oxidative stress followed by apoptosis in glioblastoma cells but not in normal human astrocytes. *Mol Cancer Res*. 2006;4(5):319–330. doi:10.1158/1541-7786.MCR-05-0061
22. Wu S, Liu X, Cheng L, et al. Protective mechanism of leucine and isoleucine against H(2)O(2)-induced oxidative damage in bovine mammary epithelial cells. *Oxid Med Cell Longev*. 2022;2022:4013575. doi:10.1155/2022/4013575
23. Pauly DF, Pepine CJ. D-Ribose as a supplement for cardiac energy metabolism. *J Cardiovascu Pharmacol Therap*. 2000;5(4):249–258. doi:10.1054/JCPT.2000.18011
24. Slawson C, Housley MP, Hart GW. O-GlcNAc cycling: how a single sugar post-translational modification is changing the way we think about signaling networks. *J Cell Biochem*. 2006;97(1):71–83. doi:10.1002/jcb.20676
25. Melnikova V, Bar-Eli M. Inflammation and melanoma growth and metastasis: the role of platelet-activating factor (PAF) and its receptor. *Cancer Metastasis Rev*. 2007;26(3–4):359–371. doi:10.1007/s10555-007-9092-9
26. Fu Y, Zhang N, Ren L, et al. Impact of an immune modulator fingolimod on acute ischemic stroke. *Proc Natl Acad Sci USA*. 2014;111(51):18315–18320. doi:10.1073/pnas.1416166111
27. Kawabori M, Kacimi R, Karliner JS, Yenari MA. Sphingolipids in cardiovascular and cerebrovascular systems: pathological implications and potential therapeutic targets. *World J Cardiol*. 2013;5(4):75–86. doi:10.4330/wjc.v5.i4.75
28. Venkataraman K, Lee YM, Michaud J, et al. Vascular endothelium as a contributor of plasma sphingosine 1-phosphate. *Circ Res*. 2008;102(6):669–676. doi:10.1161/CIRCRESAHA.107.165845
29. Gibson EL. Tryptophan supplementation and serotonin function: genetic variations in behavioural effects. *Proc Nutr Soc*. 2018;77(2):174–188. doi:10.1017/S0029665117004451
30. Puccetti P, Grohmann U. IDO and regulatory T cells: a role for reverse signalling and non-canonical NF-kappaB activation. *Nat Rev Immunol*. 2007;7(10):817–823. doi:10.1038/nri2163
31. Shi Y, Ding D, Liu L, et al. Integrative analysis of metabolomic and transcriptomic data reveals metabolic alterations in glioma patients. *J Pro Res*. 2021;20(5):2206–2215. doi:10.1021/acs.jproteome.0c00697
32. Geetha D, Attarwala N, Zhang C, et al. Serum and urinary metabolites discriminate disease activity in ANCA associated glomerulonephritis in a pilot study. *J Nephrol*. 2022;35(2):657–663. doi:10.1007/s40620-021-01095-x
33. Locasale JW, Melman T, Song S, et al. Metabolomics of human cerebrospinal fluid identifies signatures of malignant glioma. *Mol Cellular Pro*. 2012;11(6):M111.014688. doi:10.1074/mcp.M111.014688
34. Vasudevan S, Laconi E, Rao PM, Rajalakshmi S, Sarma DS. Perturbations of endogenous levels of orotic acid and carcinogenesis: effect of an arginine-deficient diet and carbamyl aspartate on hepatocarcinogenesis in the rat and the mouse. *Carcinogenesis*. 1994;15(11):2497–2500. doi:10.1093/carcin/15.11.2497
35. Rafehi M, Müller CE. Tools and drugs for uracil nucleotide-activated P2Y receptors. *Pharmacol Ther*. 2018;190:24–80.
36. Mantzourani C, Gkikas D, Kokotos A, et al. Synthesis of benzoxazole-based vorinostat analogs and their antiproliferative activity. *Bioorg Chem*. 2021;114:105132. doi:10.1016/j.bioorg.2021.105132
37. Acharya B, Chaijaroenkul W, Na-Bangchang K. Therapeutic potential and pharmacological activities of β-eudesmol. *Chem Biol Drug Des*. 2021;97(4):984–996. doi:10.1111/cbdd.13823
38. Chighizola C, Meroni PL. The role of environmental estrogens and autoimmunity. *Autoimmunity Rev*. 2012;11(6–7):A493–501. doi:10.1016/j.autrev.2011.11.027